Paper

A Simple Sensor-less Vector Control System for Variable Speed Induction Motor Drives

Student Member	Hasan Zidan	(Kyushu Institute of Technology)
Non-member	Shuichi Fujii	(Kyushu Institute of Technology)
Member	Tsuyoshi Hanamoto	(Kyushu Institute of Technology)
Member	Teruo Tsuji	(Kyushu Institute of Technology)

This paper demonstrates a new and simple speed estimation method for the induction motor (IM) drives at low speeds. This method uses the current and the input voltage in a closed loop for rotor parameter estimation. In this method, a digital system expression is considered where we assume that the rotor flux and the rotating speed are constant during a short sampling period. Simulation and experimental results demonstrate the validity of the proposed estimation algorithm for practical applications.

Keywords: Simple control, Sensor-less vector control, Parameter estimation, Digital system, Stability.

1. Introduction

Recently, there is a demand for high performance electric drives capable of accurately achieving speed command. This necessarily leads to a more sophisticated control methods to deal with such issue. Special attention was directed to induction motors because of known reasons such as size, cost, efficiency, etc. [1].

Meaning of speed sensor-less control methods of induction motors is widely recognized. There are many methods proposed already in this field [2,3,4,5]. As there are many restrictions generated by using mechanical sensors, moreover the extra expense and allocation problems that made using such sensors difficult in some cases.

Due to the rapid improvements in power devices and microelectronics and as fast microprocessors are available in the market. In this paper, a digital system expression is considered where we assume that the rotor flux and the rotating speed are constant during a short sampling period. This assumption is fairly acceptable as will be shown throughout this paper.

The proposed speed sensor-less control method valid for both low speed range and also for very low speed range. First, a traditional approach is employed; that is, stator terminal voltages and currents estimate the rotor angular speed, slip angular speed and the rotor flux. In this case, a simulation result shows that around zero speed, the slip angular velocity estimation becomes impossible since division by zero takes place. Another strategy will be shown to overcome this problem. As short sampling time is assumed, we could solve the linearized differential equations, then get an algebraic equation for the estimation of rotor parameters.

Both simulation and experimental works have validated the proposed estimation method for practical applications. In addition, the effect of the PI controller gains in the speed loop on the responses are discussed experimentally.

2. Induction Motor Model

The dynamic model of a 3 phase induction motor can be described in the stationary reference frame (α, β-coordinates) as

$$\frac{d}{dt}\begin{bmatrix} i_s \\ \phi_r \end{bmatrix} = \begin{bmatrix} a_{11} & a_{12} - j\rho\omega_r \\ a_{21} & a_{22} + j\omega_r \end{bmatrix}\begin{bmatrix} i_s \\ \phi_r \end{bmatrix} + \begin{bmatrix} b_s \\ 0 \end{bmatrix} u_s \quad \cdot (1)$$

where

$$a_{11} = -(\frac{R_s}{\sigma L_s} - \frac{1-\sigma}{\sigma\tau_r}), \quad a_{12} = \frac{L_m}{\sigma L_s L_r \tau_r},$$

$$a_{21} = \frac{L_m}{\tau_r}, \qquad a_{22} = -\frac{1}{\tau_r},$$

$$b_s = \frac{1}{\sigma L_s}.$$

R_s, R_r	:	stator, rotor resistance per phase respectively
L_s, L_r	:	stator, rotor inductance per phase respectively
L_m	:	magnetizing inductance per phase
ω_r	:	rotor angular speed
τ_r	:	rotor time constant $(= L_r/R_r)$
ρ	:	$L_m/\sigma L_s L_r$
σ	:	leakage coefficient. $(= 1 - (L_m^2/L_s L_r))$

The state and the input variables are as follows,

stator current	:	$i_s = i_{s\alpha} + j i_{s\beta}$
rotor flux	:	$\phi_r = \phi_{r\alpha} + j\phi_{r\beta}$
stator voltage	:	$u_s = u_{s\alpha} + j u_{s\beta}$

3. System Formulation

The rotor flux can be expressed in the polar coordinate as

$$\phi_r = |\phi_r| e^{j\theta} \quad \cdots\cdots (2)$$

where θ is the rotational angle, based on the assumption that the sampling period is short enough, so that the rate of change of the rotor flux is zero within the sampling period, so that

$$\frac{d}{dt}|\phi_r| = 0,$$

the derivative of (2) is

$$\frac{d}{dt}\phi_r = j\omega\phi_r$$

$\omega = \frac{d}{dt}\theta$: electrical angular speed. From (1)

$$\frac{d}{dt}\phi_r = j\omega\phi_r = a_{21}i_s + (a_{22} + j\omega_r)\phi_r$$

or

$$\phi_r = \frac{a_{21}i_s}{-a_{22} + j\omega_s} \quad \cdots\cdots (3)$$

$\omega_s = \omega - \omega_r$: slip angular velocity. The solution for the rotor flux mentioned before is valid within the sampling period. The stator current from (1) is given as

$$\frac{d}{dt}i_s = a_{11}i_s + (a_{12} - j\rho\omega_r)\phi_r + b_s u_s \quad \cdots\cdots (4)$$

By substituting the value of ϕ_r from (3) into (4), the following is achieved

$$\frac{d}{dt}i_s = a_{11}i_s + \frac{(a_{12} - j\rho\omega_r)a_{21}}{-a_{22} + j\omega_s}i_s + b_s u_s \quad \cdots (5)$$

Now let

$$A = a_{11} + \frac{(a_{12} - j\rho\omega_r)a_{21}}{-a_{22} + j\omega_s} \quad \cdots\cdots (6)$$

where

$$A = \alpha + j\beta$$

Solving (6) gives the estimation of rotor speed $\hat{\omega}_r$, slip angular speed $\hat{\omega}_s$ as will as electrical angular speed $\hat{\omega}$.

$$\hat{\omega}_r = \frac{\beta a_{22}}{a_{21}\rho} + \frac{(\alpha - a_{11})}{a_{21}\rho}\hat{\omega}_s \quad \cdots\cdots (7)$$

$$\hat{\omega}_s = -\frac{(\alpha - a_{11})a_{22} + a_{12}a_{21}}{\beta} \quad \cdots\cdots (8)$$

$$\hat{\omega} = \hat{\omega}_r + \hat{\omega}_s \quad \cdots\cdots (9)$$

The above three formulas are the general estimation equations in the proposed system. What we need now is to evaluate α and β . From (5) and (6) and assuming that the rotor speed and the slip speed are both constant during the sampling period, the following can be known

$$\frac{d}{dt}i_s = Ai_s + b_s u_s.$$

Discretizing the previous equation and and rewriting it in a real and an imaginary parts. α and β will take the following forms

$$\alpha(kT) = \frac{i_{s\alpha}((k-1)T)X(kT) + i_{s\beta}((k-1)T)Y(kT)}{c_2(i^2_{s\alpha}((k-1)T) + i^2_{s\beta}((k-1))T)}$$

$$\beta(kT) = \frac{i_{s\alpha}((k-1)T)Y(kT) - i_{s\beta}((k-1)T)X(kT)}{c_2(i^2_{s\alpha}((k-1)T) + i^2_{s\beta}((k-1)T))}$$

where

$$X(kT) = i_{s\alpha}(kT) - i_{s\alpha}((k-1)T) - c_3 u_{s\alpha}((k-1)T)$$

$$Y(kT) = i_{s\beta}(kT) - i_{s\beta}((k-1)T) - c_3 u_{s\beta}((k-1)T)$$

and

$$c_1 = e^{a_{11}T}$$

$$c_2 = (c_1 - 1)/a_{11}$$

$$c_3 = c_2/\sigma L_s$$

T : sampling period.

The above algorithm is valid for transient and steady state, but in the case of zero crossing or around zero speed, β passes through zero which means division by zero in the slip angular speed estimation (8). In order to avoid this situation, another estimation method for the slip angular speed is made as follows

$$\hat{\omega}_s = -a_{22}\frac{i^*_{sq}}{i^*_{sd}} = \frac{R_r}{L_r}\frac{i^*_{sq}}{i^*_{sd}} \quad \cdots\cdots (10)$$

where i^*_{sq} is the torque producing current command, and i^*_{sd} is the magnetizing current command. Equation (10) shows that at a very low speed or while reversing the rotational motion division by zero will not takes place, since i^*_{sd} is constant and greater than zero.

Estimation of the necessary angle for the coordinate transformations (θ) can be achieved in two ways, first, through the rotor flux estimation based on (1)

$$\hat{\phi}_{r\alpha} = \frac{a_{21}(a_{22}i_{s\alpha} + \hat{\omega}_s i_{s\beta})}{a^2_{22} + \hat{\omega}^2_s}$$

$$\hat{\phi}_{r\beta} = \frac{a_{21}(a_{22}i_{s\beta} + \hat{\omega}_s i_{s\alpha})}{a^2_{22} + \hat{\omega}^2_s}$$

again, based on (2) $\hat{\theta}$ is

$$\hat{\theta} = \tan^{-1}\frac{\hat{\phi}_{r\alpha}}{\hat{\phi}_{r\beta}} \quad \cdots\cdots (11)$$

Both the simulation and the experimental testing shows a poor response at very low speed due to the accumulation error in the rotor flux estimation, and as a result in $\hat{\theta}$, which agrees with [2].

As the electrical angular speed $\hat{\omega}$ is already estimated in (9), then θ can be estimated as follows

$$\hat{\theta} = \int \hat{\omega}\, dt \quad \cdots\cdots (12)$$

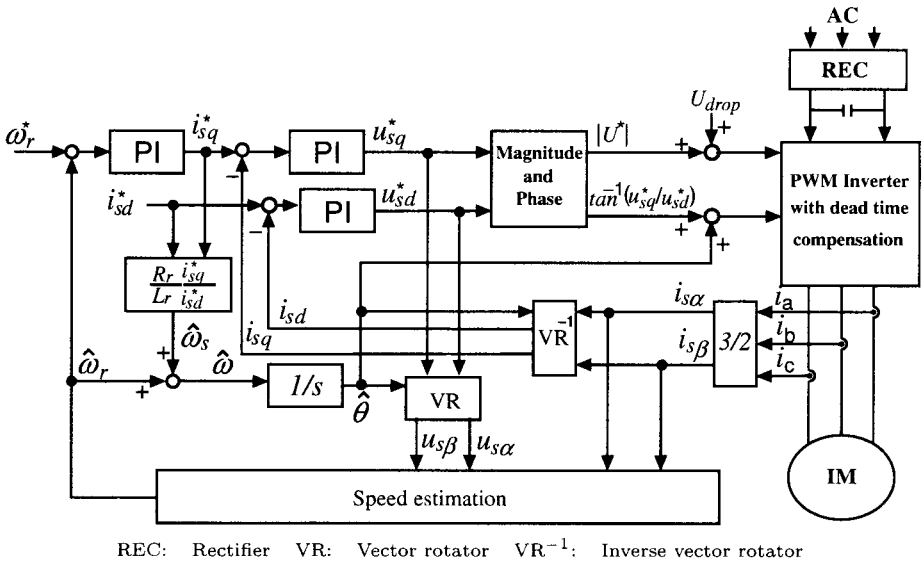

Fig. 1. Block diagram of the induction motor drive.

Table 1. Induction motor ratings and parameters.

Rated Power	0.75 kw
Rated Voltage	200 V
Number of Phase	3
Number of Poles	4
Rated Frequency	60 Hz
Line Current	3.27A
Rated Speed	1750 rpm
Rated Torque	4.09 Nm
Moment of Inertia (J)	0.04 kgm^2
Rotor type	squirrel cage
Rotor Resistance (R_r)	2.12 Ω
Stator Resistance (R_s)	2.91 Ω
Rotor Inductance (L_r)	176 mH
Stator Inductance (L_s)	176 mH
Mutual Inductance (L_m)	169 mH

4. Simulation Results

To demonstrate the effectiveness of the proposed method, a digital simulation program using MATLAB is implemented. The results hereafter are for the motor whose parameters shown in Table 1. Since the whole idea based on the assumption of the short sampling period, two cases are studied,

- Case 1: Sampling period is 1.0 ms
- Case 2: Sampling period is 0.25 ms

Under both cases the motor will start from rest. As explained in the previous section, the estimated speed and angle are given by the measured currents and the input voltage through the values of α and β. The estimated speed and the estimated angle are fed back to the system to control the motor speed.

Fig.1 shows the block diagram of the proposed speed sensor-less control method of the induction motor. Inputs to the plant are the voltages and the frequency and the outputs can be the rotor speed, the rotor position, and the torque. Moreover, our inverter can output the demanded voltage exactly as required because the voltage drop of the chips are compensated by adding the signal U_{drop} in Fig.1 and with respect to the dead time the pulse widths are modified in the PWM inverter shown in Fig.1. U_{drop} and the modification of the pulse width are determined experimentally.

Fig.2 shows the responses of α and β correspond to the speed response in Fig.3 and these are required for the derivation of $\hat{\omega}_r$.

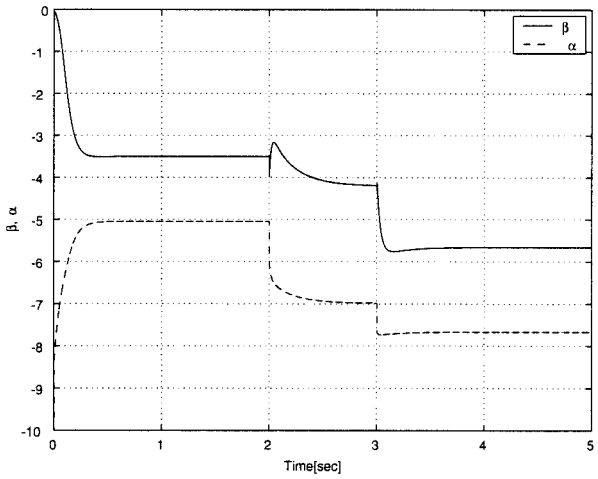

Fig. 2. α and β.

Fig.3 (a) shows the step responses for the first step change from 0.0 Hz to 2.0 Hz and the second step change from 2.0 Hz to 3.0 Hz after 3 s as reference command, where the dashed line is the estimated speed $\hat{\omega}_r$, the solid line is the motor speed ω_r . Fig.3 (b) shows the torque producing current i^*_{sq} where the load is inserted after 2 s. The sampling period used is 0.25 ms.

Fig.4 shows the error in the speed estimation for both 1.0 ms (solid line) and 0.25 ms (dashed line) as the sampling period corresponding to the responses in Fig.3. Big estimation errors are observed at 0.0 s, 2.0 s, and 3.0 s for both cases of 1.0 ms and 0.25 ms, and these are expected errors due to the inaccuracy in the assumption

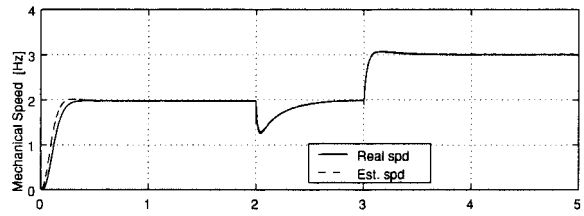

(a) Speed response to step command

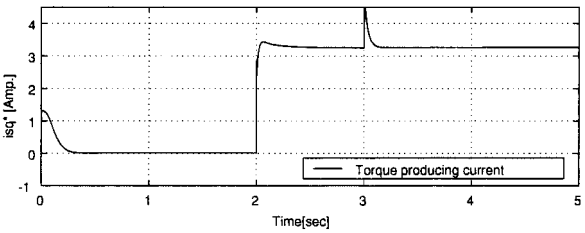

(b) Torque producing current

Fig. 3. Simulation results with T=0.25 ms as a sampling period.

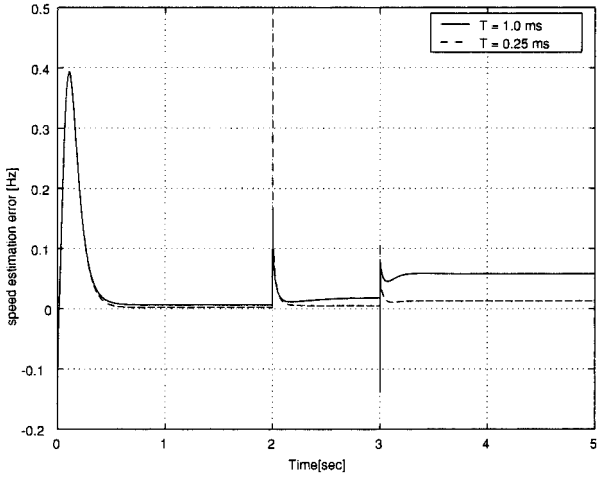

Fig. 4. Speed estimation error by varying the sampling period T.

which state that the rotor speed and the rotor flux are both constant within the sampling period. The estimation deteriorated especially with these step changes in the reference command.

Both 1.0 ms and 0.25 ms sampling period clearly shows that the proposed method can be applied to control the induction motor drives without using speed sensor. At the steady state simulation results show that a shorter sampling period results in a less estimation error as in Fig.4.

5. Experimental Results

The following are some experimental results achieved with 1.0 ms as a sampling period.

Fig.5 shows a view of the experimental system, where two similar induction motors are coupled, one is regarded as load or acts as generator. A speed sensor is used to monitor the real speed of the induction motor. Moreover, the driver (inverter) in the experimental system is adjusted to produce the exact voltage as ordered by the instruction. That is, this driver is designed to compensate the errors by dead time at the PWM control and voltage drops at switching devices.

Fig. 5. View of the experimental system.

Fig.6 shows the experimental result of the response from 0.0 Hz to 0.2 Hz (almost 6 rpm) as the speed command and no disturbance load is applied. The solid line is the real speed ω_r, dashed line is the estimated speed $\hat{\omega}_r$. Since we are dealing with a very low speed where interference and measurement error is relatively large, satisfactory result is assumed.

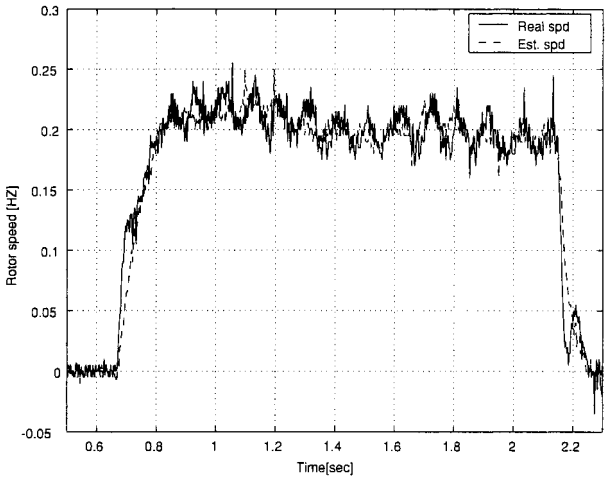

Fig. 6. Experimental results, step response of 0.2 Hz as a speed command without load insertion.

Fig.7 (a) shows the experimental result of the response from 0.0 Hz to 4.8 Hz almost 140 rpm as a speed command. The load is inserted after 6.4 s which corresponds to about 1.2 Nm. The gains are designed so as to give a faster recovery time for the disturbance load, so that a little overshoot is observed. This overshoot can be eliminated by varying the gains of the PI controllers

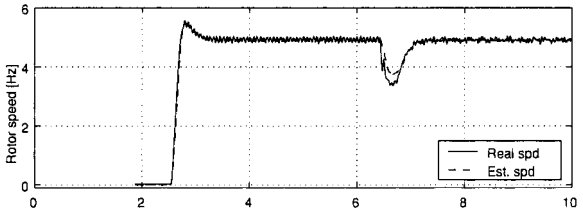

(a) Speed response to step command of 4.8 Hz

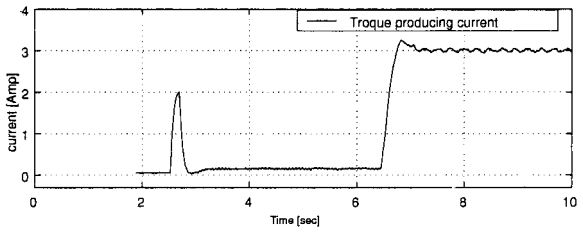

(b) Torque producing current i_{sq}^{*}

Fig. 7. Experimental results, response to load insertion.

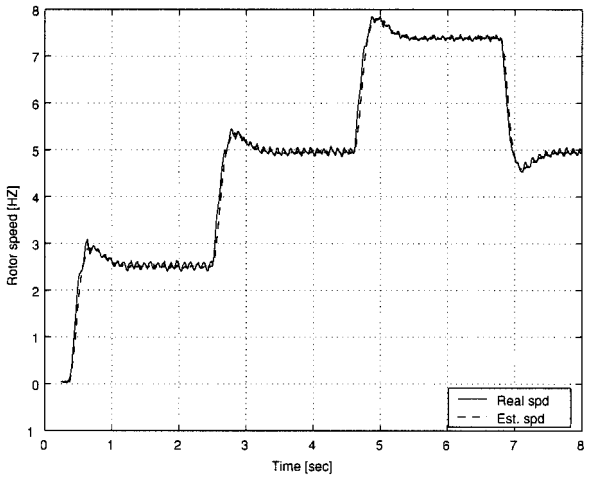

Fig. 8. Experimental results, response characteristics of the control system by varying the speed command and without load insertion.

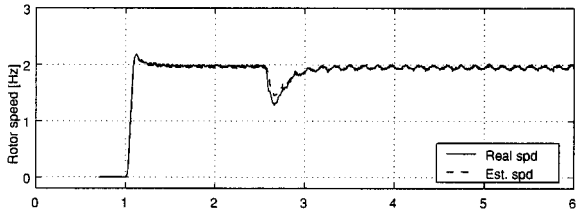

(a) Speed response to step command of 2.0 Hz

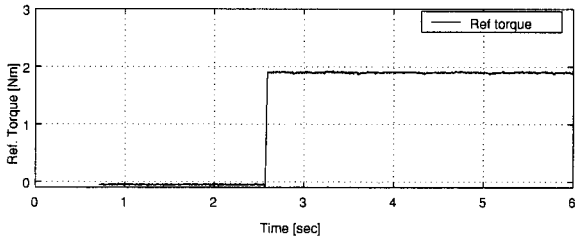

(b) Reference load

Fig. 9. Experimental results, PI controller gains designed for fast recovery time to disturbance load insertion.

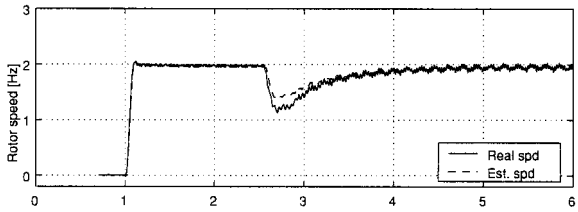

(a) Speed response to step command of 2.0 Hz

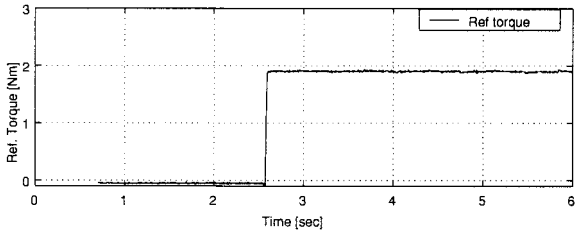

(b) Reference load

Fig. 10. Experimental results, PI controller gains designed to minimize the overshoot in the transient response.

which will be clearly demonstrated in Fig.9, Fig.10 and Fig.11. The recovery time when the load inserted is 0.6 s. Fig.7 (b) shows the torque producing current i_{sq}^{*}.

Fig.8 shows the experimental result of multi-steps [0.0 – 2.5 – 5.0 – 7.5 – 5.0 Hz (almost 0.0 – 75 – 150 – 225 – 150 rpm)] as a speed command and without load insertion. Speed estimation error is almost zero even though the reference command varies.

In order to discuss the effect of the PI controller gains in the speed loop on the responses, the following experiments are performed.

Fig.9 (a) shows the experimental result of the step response from 0.0 Hz to 2.0 Hz as a speed command. The load is inserted after 2.5 s. The PI controller gains are designed so as to give a faster recovery time for the disturbance load, so that overshoot is observed. Fig.9 (b) shows 1.9 Nm or about 50 % of the full motor torque, as a reference load torque applied to the system.

Fig.10 (a) shows the experimental result for just the same conditions as those in Fig.9 except the PI controller gains which are designed so as to minimize the overshoot. On the other hand, the response to the disturbance load is slow and a long recovery time of about 2.5 s is observed. Further more the real speed of the motor drops to a lower level than that in the previous figure. Fig.10 (b) shows the reference torque which is similar to Fig.9 (b).

Fig.11 (a) shows the same experimental result of the step response as those in Fig.9 and Fig.10. The main reason for this figure is to show that we can have fast recovery time and small overshoot in the transient response simultaneously. In this case the PI controller gains were changed just after the desired rotor speed was reached, where mainly the I gain was increased. Fig.11 (b) shows the reference torque which is the same as those in Fig.9 (b) and Fig.10 (b).

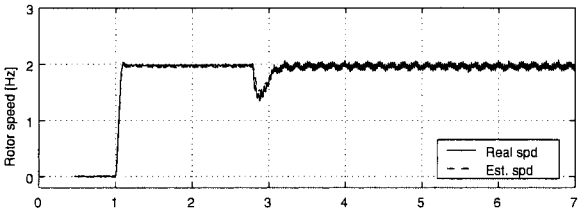

(a) Speed response to step command of 2.0 Hz

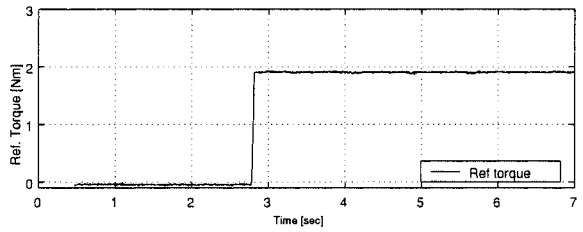

(b) Reference load

Fig. 11. Experimental results, response to load insertion and with PI controller gains variation.

6. Conclusions

The proposed estimation method has been successfully applied to control the induction motor drives without using speed sensors. Stability to a very low seed range has been demonstrated, which shows excellent performance. Since the whole idea based on a short sampling period and a faster microprocessor can realize this condition, a parameter estimation error becomes smaller and as a result improves the system response.

As was mentioned throughout this paper, direct slip estimation (8) did not achieve the desirable result due to zero divide, so that another method is used in (10). Accumulation error in the rotor flux estimation prevent us from using it for the angle estimation (11), instead, the integration was used and successfully estimated the desired angle as was mentioned in (12). Equation (10) and (12) are effective to estimate the slip angular speed and the rotational angle in both simulation and experiment.

Experimental testing shows that it is better to apply the different PI controller gains for the transient response and for the response to the disturbance load respectively.

Acknowledgment

The authors gratefully thank the valuable support from the YASKAWA ELECTRIC CORPORATION Motor Drive Section.

(Manuscript received October 18, 1999, revised May 10, 2000)

References

(1) Peter VAS, *Vector Control of AC Machines*, Clarondon press, OXFORD, 1990.
(2) Min-Huei Kim, James C. Hung, "VECTOR CONTROL SYSTEM FOR INDUCTION MOTOR WITHOUT SPEED SENSOR AT VERY LOW SPEED", Tran. of IEEE Power App., Sep. 1995.
(3) Jung-Ik Ha, Seung-Ki Sul, " Sensorless Field-Orientation Control of an Induction Machine by High-Frequency Signal Injection", Trans. of IEEE Industry Appl. Vol. 35, No. 1, Jan. 1999.
(4) H. Kubota, K. Matsuse, " Speed Sensorless Field Oriented Control of Induction Motor with Rotor Resistance Adaptation", Proc. of IEEE IAS Conf 1994.
(5) C. Attaianese, A. Perfettp, I. Marongiu, " An Observer for Speed Sensor-less Induction Motor Drive Estimating Rotor Resistance Variations", Proc. of Oct. 1994 IEEE IAS Conf.

Hasan Zidan (Student Member) was born in the West Bank, Palestine on Feb. 6, 1968. He received the B. S. from the AMTA university, Egypt in 1991. He received the M. S. from Kyushu Institute of Technology, Japan in 1998. Currently, he is a Ph. D. student in the Department of Electrical Engineering, Kyushu Institute of Technology, Japan. His research interests include adaptive control, variable structure control, and applications to AC drive systems.

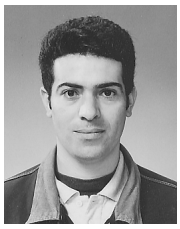

Shuichi Fujii (Non-member) was born in Yamaguchi, Japan on sep. 1969. Currently, he is in a M. Sc. student in the Department of Electrical Engineering, Kyushu Institute of Technology, Japan. His research interests include applications to AC drive systems.

Tsuyoshi Hanamoto (Member) was born in Yamaguchi, Japan on July 22, 1961. He received the B. S. and the M. S. from Kyushu Institute of Technology, Japan, in 1984 and 1986, respectively. In 1986 he joined Kobe works of Kobe Steel, Ltd. In 1990 he was engaged with the Center for Cooperative Recearch of Kyushu Institute of Technology. From 1997 to 2000 he was with the Department of Electrical Engineering. Since April 2000 he has been with the Graduate School of Life Science and Systems Engineering, where he is presently an Associate Professor. His research interests include motor control, motion control and sensorless control of AC machines.

Teruo Tsuji (Member) was born in Nagasaki, Japan on May 1940. He received the B. S., M. S., and Dr. Eng. degrees in Electrical Engineering from Kyushu University, Japan, in 1963, 1965 and 1978 respectively. Since 1968 he has been with the Department of Electrical Engineering, Kyushu Institute of Technology, where he is presently a Professor. His research interests include control, identification, and control application to magnetic levitation systems and power electronics systems